INVENTION: Multi-scale code division frequency/wavelet multiple access

INVENTORS: Urbain Alfred von der Embse

5

TECHNICAL FIELD

The present invention relates to both orthogonal frequency division multiple access OFDMA, to orthogonal Wavelet division multiple access OWDMA, to code division multiple access CDMA, and to multi-scale code division multiple access MS-CDMA, for cellular telephone and wireless data communications with data rates up to multiple T1 (1.544 Mbps), E1 (2.048 Mbps), Sonet, Ethernet, and higher (>10 Gbps), and to optical CDMA and optical OWDMA. Applications are to wire, wireless local area, wide area, mobile, point-to-point, and satellite communication networks. More specifically the present invention relates to a new and novel means for combining MS-CDMA with OFDMA, to a new and novel OWDMA which is an orthogonal multi-resolution complex Wavelet multiple access generalization of OFDMA, and to a new and novel means for combining MS-CDMA with OWDMA. This new architecture MS-CDMA OFDMA/OWDMA is an attractive candidate to replace current and future OFDMA applications and CDMA applications.

CONTENTS

BACKGROUND ART

Current OFDMA art is represented by the applications to the wireless cellular communications standards IEEE 802.11a, IEEE 802.11g, IEEE 802.15.3a, IEEE 802.16. OFDMA uses the Fourier

1

transform basis vectors as the orthogonal channelization vectors for communications with each basis vector multiplied by a symbol which is encoded with a data or pilot signal word.

The discrete Fourier transform DFT implemented as the fast Fourier transform FFT is defined in equations (1). Step 1 defines the digital sampling interval T over time, the sampling instants t=iT where i is the time index and where the sampling time 1/T is at least equal to the complex Nyquist sampling rate to prevent spectral foldover. Step 2 is the FFT of the time function Y(i) and step **3** is the inverse FFT^{-1} of the frequency spectrum X(k) which derives the original time function Y(i). Step **4** defines the NxN orthogonal complex DFT matrix E row vectors E(k) which are the DFT harmonic vectors or basis vectors or code vectors or channelization vectors. Step **5** is the complex baseband transmitted signal z(i) for one data block and is equal to the inverse FFT transform FFT^{-1} of the user symbols x(k).

Unweighted DFT encoding (1)

1 Sampling interval of DFT

|---------|------ - - - ------|---------|
t → 0   T   . . . .   (N-2)T   (N-1)T
i → 0   1   N-1   N-1

where $1/T \geq$ complex Nyquist sample rate

2 FFT of Y(i)

$$X(k) = FFT[\ Y(i)\ ]$$

$$= \Sigma_i\ E(k,i)\ Y(i)$$

$$= \Sigma_i\ exp(-j2\pi\ ki/N)\ Y(i)$$

3 FFT^{-1} of X(k)

$$Y(i) = FFT^{-1}[\ X(k)\ ]$$

$$= N^{-1}\ \Sigma_k\ E^*(k,i)\ X(k)$$

$$= N^{-1}\ \Sigma_k\ exp(j2\pi\ ki/N)\ X(k)$$

4 DFT orthogonal harmonic code matrix E

$$E = NxN\ DFT\ orthogonal\ DFT\ matrix$$

$$= [E(k,i)]\ \ matrix\ of\ elements\ E(k,i)$$

$$E(k,i) = \exp(-j2\pi ki/N) \quad \text{harmonic } k, \text{ time index } i$$

$$E(k) = \text{harmonic } k \text{ basis (code) vector}$$

$$= [E(k,0), E(k,1), \ldots, E(k,N-1)]$$

$$EE^* = N\ I$$

5

$$\langle E(k), E^*(k') \rangle = \delta(k-k')\ N\ I$$

$$\text{where} \quad I = N \times N \text{ identify matrix}$$

$$E' = \text{complex conjugate transpose of } E$$

$$\delta(k-k') = \text{Dirac delta function}$$

$$= 1 \text{ for } k=k'$$

10

$$= 0 \text{ otherwise}$$

5 Transmitted DFT complex baseband signal z(i) for one data block

$$d(k) = \text{data modulation for user } k$$

$$= \text{encoded amplitude } A(k) \text{ and phase } \varphi(k)$$

15

$$x(k) = \text{transmitted symbol encoded with } d(k)$$

$$= A(k) \exp(j\varphi(k))$$

$$z(i) = \text{FFT}^{-1}[\ x(k)\ ]$$

$$= N^{-1} \sum_k x(k)\ E^*(k,i)$$

20

OFDMA for IEEE 802.11g in reference [1] is illustrated in FIG. 1. The channelization filter h(f) **1** covers a 20 MHz frequency band **2** assigned to OFDMA. Plotted is the power spectral density PSD=$|h(f)|^2$ of this channelization filter h(f). A N=64

25   point fast Fourier transform FFT covers this band **2**. Consistant with the IEEE specification, FIG. 1 refers to the DFT which is identical to the analog Fourier transform FT since it is the sampled data version of the FT. It is convenient to consider the DFT in this invention disclosure as the digital format for the

30   FFT. The DFT frequency spectrum **3** consists of N=64 equally spaced filters **4** across this 20 MHz band. Filter spacing is equal to the DFT output rate 1/NT = 0.3125 MHz = 20MHz/64. The DFT time pulse p(t) **5** is NT=3.2µs in length and the total DFT period **6** is 4.0µs which allows a 0.8µs guard time for p(t).

3

Throughout this invention disclosure it will be understood that the FFT fast algorithm will always be used to implement the DFT and the inverse FFT^{-1} fast algorithm will always be used to implement the inverse DFT^{-1}.

5   **OFDMA transmitter encoding** of the OFDMA waveform in FIG.1 is defined in equations (2). Step **1** lists the parameters and definitions and step **2** defines the time domain weighting. Step **3** is the complex baseband transmitted signal z(i).

10   **OFDMA encoding for transmitter**   (2)

    1 Parameters and definitions from **1** in equation (1)

      and

        h(i)   = 20 MHz band filter impulse response

        p(i)   = impulse response of the DFT waveform

15   .   = real weighting function in **6** in FIG. 1

        N   = 64 point DFT

        1/T   = 30 MHz sample rate for DFT

             ≥ complex Nyquist rate

        NT   = 3.2µs DFT length

20   1/NT = 0.3125 MHz DFT output rate

           = DFT channel separation

           = DFT tone spacings

      52 channels are used: 4 pilot, 48 data

      12 guard band channels for rolloff of the h(k)

25   **2 Pulse p and band filter h weighting for DFT basis vectors**

      p = p©h, convolution of p and h

        = filter transfer function in time domain

          for the combined h and p filters

        = [p(0), p(1), . . ., p(N-1)]

30   **3 Transmitted OFDMA encoded baseband signal z(i)**

      for one data block

        d(k)   = data modulation for user k

            = encoded amplitude A(k) and phase φ(k)

        x(k)   = transmitted symbol encoded with d(k)

$$= A(k) \ \exp(j\varphi(k) \ )$$
$$z(i) \ = \ FFT^{-1}[\ \underline{p}(i) \ x(k) \ ]$$
$$= \ N^{-1} \ \Sigma_k \ \underline{p}(i) \ x(k) \ E^*(k,i)$$

5   OFDMA for IEEE 802.11g has the strict orthogonality of the DFT(FFT) replaced by cross-correlations between the 48 channel tones and other impacts due to the band channelization and pulse weighting p©h plus the time errors Δt and frequency errors Δf from synchronization errors, multi-path, propagation, and

10   terminal stresses. These impacts on orthogonality are low enough to allow OFDMA support higher values for the symbol signal-to-noise ratio S/N in the detection band that are required for higher order symbol modulations. The highest order symbol modulation currently is 64 state quadrature amplitude modulation

15   64QAM corresponding to 6 bits per symbol where $6=\log_2(64)$ and $\log_2(o)$ is the logarithm to the base 2. With rate 3/4 convolutional coding the highest information rate is 4.5 bits/symbol = 6x3/4. Required S/N at a BER=1.0e-6 is approximately S/N~19 dB.

20   OFDMA for IEEE 802.11g provides 48 channels over a 20 MHz frequency band at a symbol rate equal to 0.25 MHz=1/4.0 μs from **6** in FIG. 1 and for a maximum information rate equal to 4.5 bits/symbol this equals a burst rate of 54 MBps = 4.5x48x0.25. Some spread spectrum properties are realized by hopping the 20

25   MHz band, shuffling the channel assignments over the 48 available channels for a user assigned to several channels in order to spread his transmissions over the band, and for "flash" ODFMA by a random hopping of each user channel across the 48 available channels within the band.

30   **OFDMA receiver decoding** of the OFDMA waveform in FIG.1 is defined in equations (3) for the receiver. Step **1** identifies the parameters and definitions and defines the convolution R(i)= $\underline{p}$©$\underline{p}$ of the time domain weighting $\underline{p}$ with itself in the matched filter

receiver. Step **2** derives the estimates of the transmitted symbols by implementing matched filter detection in the receiver.

        OFDMA decoding for receiver   (3)

1 Parameters and definitions are defined in **1,2** in equations (2) together with

$$R(i) = \text{convolution of } \underline{p} \text{ with } \underline{p}$$
$$= \underline{p} © \underline{p}$$

2 OFDMA decoding for one data block derives estimates $\hat{x}(k)$ of x(k) from the receiver estimates $\hat{z}(i)$ of z(i)

$$\hat{x}(k) = FFT[\ \hat{z}(i)©\underline{p}\ ]$$
$$= \Sigma_i\ \hat{z}(i)©\underline{p}\_E(k,i)$$

        Current CDMA spread spectrum art is illustrated by the waveform in FIG. 2 which describes the waveform for full band CDMA communications over the band B **9** which is the output range **8** of the band filter h(f) **7**. The CDMA chip rate $1/T_c$ **12** is less than the available frequency band B to allow the chip frequency spectrum p(f) **10,11** to roll off. As defined **9** in FIG. 2 the band B and chip rate are related by equation B=(1+ α)/T_c where α is the bandwidth expansion factor close to α=0.25 for high performance communications. Frequency spectrum p(f) **10** for the CDMA communications is essentially equal to the Fourier transform of the CDMA time pulse p(t) **13**. The representative time pulse p(t) is a square-root raised cosine pulse which is typically used for high performance communications to obtain a reasonably flat spectrum with a sharp rolloff at the edges to enable the chip rate $1/T_c$ to be reasonably close to the available frequency band B.

        Chip rate $1/T_c$ is the CDMA total symbol rate. The users could be at different data rates but this and other architectural
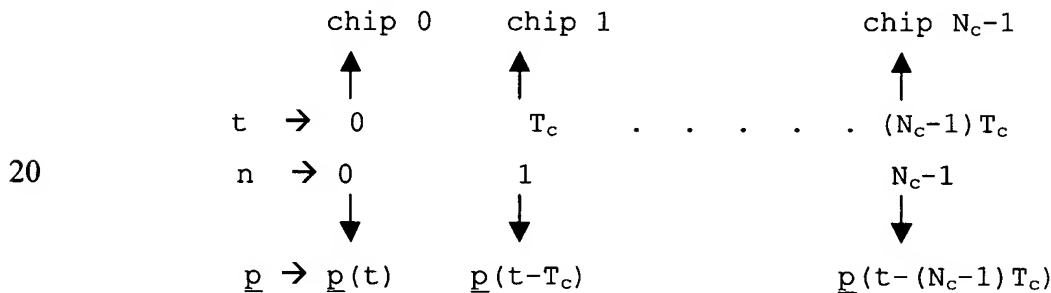
variations do not limit the scope of this invention. Power is uniformly spread over the CDMA pulse waveform spectrum p(f).

It is self evident to anyone skilled in the CDMA communications art that these communications mode assumptions are both reasonable and representative of the current CDMA art and do not limit the applicability of this invention.

CDMA encoding of the waveform in FIG. 2 for the transmitter is defined in equations (4). Steps **1,2** define the CDMA transmission and parameters. Step **3** defines the user symbol x(u). Step **4** is the set of Walsh orthogonal channelization codes w(u) and step **5** is the pseudo-random PN covering or spreading code. Step **6** defines the complex baseband signal z(t) as the waveform $\underline{p}(t-nT_c)$ multiplied by the encoded sum over u and n.

CDMA encoding for transmitter (4)

1 CDMA transmission

	chip 0	chip 1		chip N_c-1
	↑	↑		↑
t →	0	T_c	. . . . .	$(N_c-1)T_c$
n →	0	1		N_c-1
	↓	↓		↓
$\underline{p}$ →	$\underline{p}(t)$	$\underline{p}(t-T_c)$		$\underline{p}(t-(N_c-1)T_c)$

where $\underline{p}(t-nT_c) = p(t-nT_c) ©h(t)$
                = convolution of $p(t-nT_c)$ and h
                = filter transfer function in time domain
                    for the combined $p(t-nT_c)$ and h filters

2 Parameters and definitions
        N_c = Number of users and orthogonal code chips
        T_c = CDMA chip length or repetition interval
        $1/N_cT_c$ = User symbol rate

3 User complex signal x(i)
        d(u)   = data modulation for user u
                 = encoded amplitude A(u) and phase φ(u)

$$x(u) \quad = \text{transmitted symbol encoded with } d(u)$$
$$= \dot{A}(u) \, \exp(j\varphi(u)\ )$$

4   Walsh orthogonal channelizaation code matrix W

$$W \qquad = \text{Code matrix,} \quad N_c \text{ rows of } N_c \text{ code vectors}$$
$$= [\ W(k,n)\ ] \quad \text{matrix of elements } C(k,n)$$
$$W(u,n) = +/-1, \text{ chip n of vector u}$$
$$W(u) \quad = \text{code vector u, row k of W}$$
$$= [W(u,0),\ W(u,1),\ \ldots\ ,W(u,N_c-1)]$$

5   PN covering (spreading) code P(n) for chip n

$$P(n) \quad = \exp(j\varphi(n))$$

6   Transmitted CDMA complex baseband signal z(t)

$$z(t) \quad = N_c^{-1} \, \Sigma_u \, \Sigma_n \, P(n)W(u,n)x(u) \, \underline{p}(t-nT_c)$$

CDMA decoding of the waveform in FIG. 2 for the transmitter is defined in equations (5).   Step **1** defines the convolution $R(n,n-n')$ of the CDMA pulse waveform with itself in the matched filter receiver.   Steps **2,3**   are   the   Walsh, PN decoding properties. Step **4** uses the matched filter detection theorem to derive the estimates of the transmitted symbols.

CDMA decoding for receiver $\qquad\qquad\qquad$ **(5)**

1   Parameters and definitions are defined in

$\qquad$ **1,2,3** in equations (4) together with

$\qquad$ $R(n,n-n')$ = convolution of $\underline{p}(t-nT_c)$ with

$\qquad\qquad\qquad$ $\underline{p}(t-n'T_c)$ evaluated at the receiver

$\qquad\qquad\qquad$ detection times $t=nT_c$

$\qquad\qquad$ $= R(n)\ \delta(n-n')$

$\qquad\qquad$ $= R(n) \quad$ for $n=n'$

$\qquad\qquad$ $= 0 \quad$ otherewise

2   Walsh decoding of channelizaation codes W(k)

$\qquad$ $WW^{\star} \quad = N_c\ I$

$\qquad$ where $\quad I\ = N_c \times N_c$ identify matrix

$\qquad\qquad$ $W^{\star} = $ conjugate transpose of W

8

$$<W(k),W(k')> = N\ \delta(k-k')$$

3   PN decoding

$$P(n)P^*(n) = 1 \quad \text{for all } n$$

$$\text{where} \quad P^* = \text{complex conjugate of } P$$

4   CDMA decoding

$$\hat{x}(k) = \Sigma_n\ P^*(n)W^*(k,n)\ \hat{z}(t)\copyright\underline{p}(t-nT_c)$$

It should be obvious to anyone skilled in the communications art that these example implementation algorithms in equations (1),(2),(3),(4),(5) clearly define the fundamental OFDMA and CDMA signal processing relevant to this invention disclosure and it is obvious that this example is representative of the other possible signal processing approaches.

For cellular applications the encoding algorithms for the transmitter describe the implementation of OFDMA and of CDMA encoding and are the transmission signal processing applicable to this invention for both the hub and user terminals, and the decoding algorithms for the receiver describes the corresponding OFDMA and CDMA receiving signal processing for the hub and user terminals for applicability to this invention.

For optical communications applications the microwave processing at the front end of both the transmitter and the receiver is replaced by the optical processing which performs the complex modulation for the optical laser transmission in the transmitter and which performs the optical laser receiving function of the microwave processing to recover the complex baseband received signal with the remainder of the signal processing functionally the same for the OFDMA and for the CDMA encoding transmitter and functionally the same as described for the OFDMA and CDMA receiving signal processing receiver.

9

SUMMARY OF INVENTION

This invention introduces the new OWDMA communications technology which implements orthogonal multi-resolution complex Wavelet division multiple access and is a multi-resolution complex Wavelet generalization of OFDMA, introduces the new application of the multi-scale code division multiple access MS-CDMA architecture which integrates MS-CDMA with OFDMA and with OWDMA, and introduces the variable gain control over frequency.

The new OWDMA forms a uniform set of contiguous orthogonal filters across the available frequency band in one of the numerous available architectural options and which implements a polyphase filter bank across the available frequency band with the basic property that the filters are orthogonal. Each filter defines a OWDMA channel for communications. Similar to OFDMA, the symbol rate within each channel is equal to the channel separation 1/NT where N is the number of channels, 1/T is the frequency band, and NT is the symbol-to-symbol separation and which is made possible by using multi-resolution complex Wavelet channelization filters developed in reference [2]. OWDMA filters are orthogonal in frequency which means their frequency spectrums are non-overlapping, and they have flat spectrums across the channel.

OWDMA orthogonality only requires frequency synchronization whereas OFDMA orthogonality requires both time and frequency synchronization which means that time synchronization errors on the user communication channels for the return links to the hub or access point for cellular communications does not degrade the orthogonal separation between the channels as they will for OFDMA.

Sensitivity to frequency synchronization errors is less for OWDMA primarily because of the non-overlapping of the frequency spectrums. The overall tolerance to user-to-user imbalances on the return communications channels is better for OWDMA primarily because their design keeps the frequency spectrums from overlapping in the presence of real operational conditions with

10

synchronization errors.   This allows the forward communications link to support a power imbalances between channels to mitigate differing ranges and path losses at the user antennas.

Application of multi-scale code division multiple access
5   MS-CDMA in reference [2] provides a means to implement the new hybrid-Walsh orthogonal CDMA codes in reference [4] over the OFDMA/OWDMA channels by spreading the CDMA within each channel and over all of the channels such that each user can be spread over the complete band. This keeps the chip rate equal to 1/NT
10   while maintaining the spreading over the fullband 1/T and allows the band Tx power to be independently controlled in frequency. These two CDMA scales 1/NT,1/T are generated by MS-CDMA in combination with the OFDMA/OWDMA channelization filter banks. The 1/T scale is to combat fading and interference similar to the
15   current CDMA, and the 1/NT scale is for acquisition, synchronization, and protection against multi-path and provides the flexibility for band power control to provide a frequency diversity communications improvement.

Variable control over the frequency B can be implemented by
20   partitioning the CDMA over the channels into separate groups and assigning an independent power level to each group of channels. OWDMA readily supports differences in power levels between adjacent channels.   Power control is desirable to support differences in quality of service SoC, range losses , and path
25   loss.

It should be obvious to one familiar with the CDMA communications art that the number of scales could be a larger number than the two used in this invention disclosure and the multi-resolution complex Wavelet design for OWDMA supports the
30   partitioning of the frequency band 1/T into several frequency scales for the channelization filters, supports individual multi-resolution complex Wavelet packets for communications in the time-frequency domain and which can be integrated into the MS-CDMA, and supports separate and segmented communications bands
35   simultaneously.

BRIEF DESCRIPTION OF DRAWINGS

FIG. 1 is a description of the OFDMA waveform in the frequency and time domains over a 20 MHz band for the IEEE 802.11g standard.

FIG. 2 is a description of the CDMA waveform in the frequency and time domains over a band B.

FIG. 3 is a description of the OWDMA waveform in the frequency and time domains over a band B.

FIG. 4 is a description of the design requirements on the multi-resolution complex Wavelet PSD=$|\psi(f)|^2$.

FIG. 5 is a representative baseband frequency response for the multi-resolution complex Wavelet filter and the square-root cosine filters for the bandwidth expansion factors =0.22, 0.40.

FIG. 6 is a representative implementation of MS-CDMA OFDMA/OWDMA encoding for transmitter.

FIG. 7 is a representative implementation block diagram for the MS-CDMA OFDMA/OWDMA transmitter.

FIG. 8 is a representative implementation of MS-CDMA OFDMA/OWDMA encoding for the receiver.

FIG. 9 is a representative implementation block diagram for the MS-CDMA OFDMA/OWDMA receiver.

DISCLOSURE OF INVENTION

This invention introduces the new orthogonal multi-resolution complex Wavelet division multiple access OWDMA communications technology which is a multi-resolution complex Wavelet generalization of OFDMA, introduces the new multi-scale code division multiple access MS-CDMA architecture to integrate MS-CDMA with OFDMA, and introduces the new MS-CDMA architecture to integrate MS-CDMA with OFDMA,

OWDMA uses the multi-resolution complex Wavelet waveform developed in reference [2] to generate multi-rate orthogonal filter banks and waveforms to support communications at the critical symbol rate equal to a combined 1/T symbols per second for a 1/T Hz frequency band. The critical symbol rate is the Nyquist sample rate and corresponds to no excess bandwidth $\alpha=0$ in the equation $B=(1+\alpha)/T$ which can be rewritten as the bandwidth-time product $BT=(1+\alpha)$ that relates filter bandwidth B and the symbol rate 1/T for communications supported by this filter. For the OFDMA filter in FIG. 1 it is observed $BT=1+\alpha=64/52=1.33$ corresponding to $\alpha=0.33$ since 52 of the 64 DFT filters generated are used and for the CDMA filter in FIG. 2 it is observed that the bandwidth-time product is about $BT=1.25$ corresponding to $\alpha=0.25$ for the 3G CDMA cellular communications systems.

Multi-resolution complex Wavelet design algorithms were developed in reference [2] as a means to design polyphase multirate filters, quadrature mirror filters (QMF), perfect reconstruction filters, Wavelet iterated filter banks, and Wavelet tiling of the time-frequency t-f space. Prior to the invention of multi-resolution complex Wavelet design algorithms, theorectical studies had not yielded useful realizable filters for system applications implementing these architectures as summarized by the digital filtering and polyphase research in references [5].[6] and the Wavelet research as summarized in the references [7],[8],[9],10],[11].

Multi-resolution complex Wavelets defined in equations (6), (7),(8) expand the Wavelet analytical formulation to include a frequency variable which specifies the center frequency of our new Wavelets and performs a frequency translation of the real
5   mother Wavelet to this center frequency. Currrently, Wavelets are real functions of the scale and translation parameters. Multi-resolution complex Wavelets are functions of these parameters plus the frequency variable. This new concept of frequency as an additional parameter provides an added degree of flexibility and
10 together with the Fourier domain design approach provide an entirely new means for deriving these new waveforms as generalization of the traditional real Wavelets and their modification to include the added frequency parameter. With frequency translation as the additional parameters the analytical
15 formulation of these new waveforms as a function of the baseband or mother waveform centered at dc(dc refers to the origin f=0 of the frequency space) is given in equations (6).

Equations (6) introduce the new multi-resolution complex Wavelets. Step **1** in equations (6) is the definition for the
20 continuous real Wavelet over the time-frequency t-f space from reference [7],[9],[12] where ψ(t) is the Wavelet which is a waveform of finite extent in time t and frequency f over the t-f space, Wavelet parameters a,b are the Wavelet dilation and translation respectively or equivalently are the scale and shift.
25 The ψ(t) without the indices a,b is the mother Wavelet which is a real and symmetric localized function in the t-f space used to generate the doubly indexed Wavelet ψ(t|a,b) where ψ(t|a,b) reads the ψ is a function of time t for the parameters a,b. Scale factor $|a|^{-1/2}$ has been chosen to keep the norm of the Wavelet
30 invariant under the parameter change a,b. Norm is the square root of the energy of the Wavelet response. The Wavelets ψ(t|a,b) and ψ(t) are localized functions in the t-f space which means that both their time and frequency lengths are bounded.

Step **2** in equations (6) defines the digital Wavelet which is a Wavelet over the digital t-f space corresponding to digitization of the t-f space at the 1/T analog-to-digital A/D rate where T is the interval between digital samples and "i' is
5   the index over the digital samples. Time "t" for the continuous Wavelet in **1** is replaced by the equivalent digital sample number "i" corresponding to t=iT at sample i. Wavelets in digital t-f space have an orthogonal basis that is obtained by restricting the choice of the parameters a,b to the values $a=2^{-p}$, $b=qN2^p$
10   where p,q are the new scale and translation parameters and N is

New multi-resolution complex Wavelets   **(6)**

1 Current continuous Wavelet as a function of the
    mother Wavelet at dc

15           $\psi(t|a,b) = |a|^{-1/2} \psi((t-b)/a)$
    where a,b are the dilation,shift parameters

2 Current digital real Wavelet
    Digital Wavelet shift q and scale p
         $a = 2^p$

20          $b = q N 2^p$
    Digital Wavelet as a function of mother Wavelet
         $\psi(i|p,q) = 2^{-p/2} \psi(2^{-p} i-qN)$
    where N = number of samples over the Wavelet
         spacing or repetition interval

25   T_s = NT   wavelet spacing
         i   = digital sampling index
         T   = digital sampling interval
         t   = iT   time index at digital sample i

3 Our new digital multi-resoltion complex Wavelet
30   is a function of the mother Wavelet at dc
    3.a) Generalized complex format
         $\psi(i|p,q,k) = 2^{-p/2} \psi(2^{-p} i-qN) \exp[j2\pi f_c(p,k) 2^{-p}iT]$
    3.b) Multi-rate filter complex format
         $\psi(i|p,q,k) = 2^{-p/2} \psi(2^{-p} i-qN) E*(k2^p, 2^{-p}i)$

4 Orthogonality equations for our new digital complex Wavelet

$$\Sigma_i \, \psi(i|p,q,k) \, \psi^*(i|p',q',k') = N \quad \text{iff } p=p', q=q', k=k'$$
$$= 0 \quad \text{otherwise}$$

5 New digital complex Wavelet for a uniform filter bank
as a function of the mother Wavelet at dc

$$\psi(i|p=0,q,k) = \psi(i-qN) \, E^*(k,i)$$

the spacing or repetition interval $T_s=NT$ of the Wavelets (which from a communications viewpoint are symbols) at the same scale p. Wavelets at p,q are related to the mother Wavelet by the equation in **2** where the mother Wavelet is a real and even function of the sample coordinates and which follows directly from **1** for the continuous t-f space.

Steps **3,4** in equations (6) define our new Wavelet in the digital t-f space and their orthogonality properties. Our new Wavelets are complex generalizations of Wavelets in t-f space which enable them to be useful for communications and radar applications. This generalization is accomplished **1)** by the addition of a frequency translation parameter k which controls the frequency offset of the Wavelet, **2)** by generalizing the Wavelet weighted orthonormality properties in step **4** to apply to waveforms over the time translation q and over the scales p with the inclusion of the frequency translation and where ψ^* is the complex conjugate of ψ and is required in the orthogonality equations since the multi-resolution complex Wavelet ψ becomes complex with the addition of harmonic k, and **3)** by their characterization and design in the Fourier domain. The frequency parameter k controls the frequency translation $\exp[j2\pi f_c(p,k)2^{-p}iT]$ in **3** for the generalized format and the frequency translation $E^*(k2^p, 2^{-p}i)$ in **3** for the multi-rate filter format. With this frequency translation the analytical formulation **3** of these new Wavelets is given as a function of the baseband or mother waveform centered at dc corresponding to k=0. Purpose of

the frequency index k is to identify the center frequencies of the waveforms at the scale p and time translation q in the t-f space. The generalized center frequency $f_c(p,k)$ of the frequency translated dc waveform at scale p and frequency index reduces to

5    $f_c(p,k) = k2^p/NT$ for application to multi-rate filters.

Step **5** in equations (6) defines the equations for our new Wavelet for a uniform polyphase filter bank which is one of several OWDMA candidate architectures. Our new Wavelets in **5** are the impulse responses of the corresponding digital symbols

10   encoded with digital data for transmission which is the synthesis filter bank in polyphase theory, and are the filter bank detection impulse responses for recovery of the transmitted digital symbols by the analysis filter bank in polyphase theory assuming matched filter detection. The digital filters are

15   observed to be the DFT's of the mother wavelets similar to the construction of the OWDMA in equations **3** in equations (2) upon replacing the OWDMA pulse waveform p̲ with the mother Wavelet $\psi(i-qN)$ in **5** and setting q=0 corresponding to the symbol at t=0.

Equations (7) derive the multi-resolution complex Wavelet
20   **as a function of the Fourier design coordinates.** Design algorithms provide a means to design the mother Wavelet in the Fourier frequency domain to fit the communications and radar specifications. From this mother Wavelet, the Wavelets at the appropriate scales {p,q,k} are easily found as demonstrated in

25   **3,5** in equations (6). Design in the frequency domain means the design coordinates specifying the Wavelet are Fourier frequency harmonics or coordinates. Step **1** list the parameters and coordinates and step **2** define the Fourier harmonic frequency design coordinate.

30   Step **3** is the DFT representation from equations **3** in equations (1) of the real mother Wavelet $\psi(i)$ as a function of the DFT Fourier harmonic coefficients $\{\psi(k')\}$. Step **4** derives the equation for the multi-resolution complex Wavelet as a

function of the DFT Fourier harmonic coefficients by substituting **3** in equations (7) into **3** in equations (6).

  Digital multi-resolution complex Wavelet is a   **(7)**

5   **function of the Fourier harmonic design coordinates**

  1 Parameters and coordinates

   ψ $= \psi(i)$ mother Wavelet

     $= \psi(i\,|\,p=0, q=0, k=0)$

   N' $=$ length of the mother Wavelet $\psi(i)$

10 $= NL+1$

   N $=$ sampling interval of ψ

    $=$ spacing of ψ for orthogonality

   L $=$ length of ψ in units of M

   T $=$ spacing of digital samples

15 $T_s = N'T$ length of ψ in seconds

  2 Fourier harmonic frequency design coordinates

   $\psi(k')$ $=$ value of the Fourier design harmonic $k'/N'T$

     $=$ Fourier harmonic design coordinate value

   $\{k'\}$ $=$ set of harmonic design coordinates

20   for $k' = 0, +/-1, \ . \ . \ .$

     corresponding to harmonics $\{k'/N'T\}$

  3 Multi-resolution real mother Wavelet definition

   $\psi(i) = \Sigma_{k'} \ \psi(k') \ E^*(k', i)$

  4 Multi-resolution complex Wavelet definition

25 $\psi(i\,|\,p, q, k)$

   $= 2^{-p/2} \Sigma_{k'} \psi(k') \ E^*(k'/L+k2^p, 2^{-p}(i-qN))$

  Several fundamental properties follow directly from the frequency design approach in equations **4** in equations (7). It is

30 demonstrated in reference [2] that our multi-resolution complex Wavelets are implemented with our design in the Fourier domain and our multi-resolution complex Wavelet design remains invariant under scale changes. It is demonstrated in reference [2] that the

Fourier frequency domain design in equations **3** in equations (7) remains invariant for all parameter changes and in particular for all scale changes.

Multi-resolution complex Wavelet design algorithms are illustrated by a representative least-squares LS design for a OWDMA polyphase uniform filter bank in FIG. 3. There are two categories of LS algorithms and these are the eigenvalue and the gradient search that respectively can be reduced to algorithms equivalent to the original eigenvalue [13] and Remez-exchange [14] waveform design algorithms for application to a uniform filter bank.

FIG.3 is an example of an orthogonal multi-resolution complex Wavelet division multiple access OWDMA Wavelet polyphase filter bank over the band B by setting N in **5** in equations (6) equal to the N in **17** in FIG. 3. The band channelization filter is a roofing filter h(f) **14** that covers the B frequency band **15** assigned to OWDMA. Unlike its use in FIG. 1 for the OWDMA with B=20 MHz this filter is intended to be flat over the frequency band B of interest and with a bandwidth **18** equal to 1/T > B. Plotted is the power spectral density PSD=$|h(f)|^2$ of this channelization filter h(f). The h(f) output is digitized at the sample rate 1/T to form the OWDMA multi-resolution complex Wavelet polyphase filter bank **16** which are uniformly spaced **17** at 1/NT Hz over the 1/T frequency band 1/T. This digital sample rate 1/T is sufficiently large to allow the use of the shaded OWDMA filters in **17** in FIG. 3 for communications over the band B **18** with no excess bandwidth α=0 unlike the OFDMA in FIG. 1 which has α=0.33 and CDMA in FIG. 2 with α=0.25.

This OWDMA polyphase filter bank is ideally decimated which means the filter output multi-resolution complex Wavelet sample rate $1/T_s$ is equal to the channel-to-channel spacing T_s=NT equivalent to stating that there is no excess bandwidth α=0 within the filter bank. A representative **19** OWDMA multi-resolution complex Wavelet ψ for L=8 is plotted in **20** as a

19

function of the time offset expressed in units of the multi-resolution complex Wavelet spacing NT. This ψ was designed by the eigenvalue category of LS design algorithms. Our design for this topology is immediately applicable to an arbitrary set of

5   multi-resolution OWDMA filters through the scaling equations **3,4** in equatioins (7) which gives the design of our Wavelet at arbitrary scales in terms of our design of the mother Wavelet.

Multi-scale mother Wavelet ψ design for the OWDMA polyphase filter bank in FIG.3 starts by using the frequency design

10   template in FIG. 4 to construct the LS error metrics as a function of the DFT frequency design coordinates $\{\psi(k')$ in **2** in equations (7) which define the mother Wavelet in **3** in equations (7). Next minimization search algorithms are developed and used to find the values of $\{\psi(k')$ that minimize the weighted sum of

15   these LS design error metrics equal to the cost function J in equations (8) for the LS design. Minimizing J with respect to the $\{\psi(k')$ gives the design values of $\{\psi(k'\}$ for constructing the mother Wavelet in equations **3** in equations (7).

Equations (8) define the LS cost function J constructed

20   with the LS metrics with the aid of the frequency design template in FIG. 4. Step **1** define the LS error metrics which are the passband error metric $\mu(1)$, stopband error metric $\mu(2)$, quadrature mirror filter QMF error metric $\mu(3)$, intersymbol interference error metric $\mu(4)$, and the adjacent channel

25   interference error metric $\mu(5)$.

LS cost function J for designing $\psi(i)$ **(8)**

1   LS metrics

$\mu(1)$ = passband LS error metric measures the LS

30   error of the passband ripple **24** in FIG.4

$\mu(2)$ = stopband LS error metric measures the

            stopband atteunation **28** in FIG. 4

$\mu(3)$ = quadrature mirror filter QMF LS error

20

metric measures the flatness of the sum
of two contiguous filters over the
deadband **31** in FIG. 4

$\mu(4)$ = orthogonality LS error metric measures the
intersymbol interference ISI between
overlapping Wavelets of different wymbol

$\mu(5)$ = orthogonality LS error metric measures the
adjacent channel interference ACI from
nearest neighbor channels

2 Metric weighting

$w(n)$ = metric weight for error metrics n=1,2,3,4,5 in **1**
≥ 0

such that $\Sigma_n\ w(n) = 1$

3 Cost function J

$J = \Sigma_n\ w(n)\ \mu(n)$

FIG. 4 is the frequency design template for the power
spectral density PSD=$|\psi(f)|^2$ of the multi-resolution complex
Wavelet and defines the parameters of interest for the passband
metric $\mu(1)$ and stopband metric $\mu(1)$ in step **1** in equations (8).
Passband **21** of the wavelet PSD=$|\psi(f)|^2$ is centered at dc (f=0)
since we are designing the mother Wavelet, and extends over the
frequency range ω_p extending from $-\omega_p/2$ to $+\omega_p/2$ **22** in units of
the radian frequency variable $\omega=2\pi fT$ **23** where T is the
digital sampling interval defined in FIG. 3. The frequency space
extends over the range of $\Delta f=-1/2T$ to $\Delta f=+1/2T$ which is the
frequency range in FIG 3 and the mother Wavelet is at the center
of the frequency band. Quality of the PSD=$|\psi(f)|^2$ over the
passband is expressed by the passband ripple **24**. Stopband **25**
starts at the edge **26** of the passbands of the adjacent channels
+/-$\omega_a/2$ **26** and extends to the edge of the frequency band $\omega=+/-$
π **27** respectively. Stopband attenuation **28** at +/-$\omega_a/2$
measures the PSD=$|\psi(f)|^2$ isolation between the edge of the

21

passband for the mother Wavelet and the start of the passband for the adjacent Wavelet channel centered at $+/-\omega_s$ **29**. Rolloff **30** of the stopband is required to mitigate the spillover of the Wavelet channels other than the adjacent Wavelet channels, onto

5   the mother Wavelet channel. Deadband or transition band **31** is the interval between the passbands of contiguous Wavelet channels, and is illustrated in FIG. 4 by the interval from $\omega_p/2$ to $\omega_a/2$ between the mother Wavelet channel and the adjacent Wavelet channel at ω_a. Waveform sample rate ω_s **32** is the

10 waveform repetition rate. For the LS example algorithm, the waveform sample rate is equal to the channel-to-channel spacing for zero excess bandwidth. Therefore, $1/T_s= \omega_s/2\pi T=1/MT$ which can be solved to give $\omega_s=2\pi/M$ for the radian frequency sampling rate of the filter bank which is identical to the Wavelet

15 repetition rate.

Equations (8) step **1** QMF LS error metric $\mu(3)$ expresses the requirement on the deadband that the PSD's from the contiguous channels in FIG. 4 add to unity across the deadband **31** [ω_p, ω_s] in FIG. 4 in order that the Wavelets be QMF filters.

20 Equations (8) step **1** ISI and ACI error metrics $\mu(4),\mu(5)$ are orthonormality metrics that measure how close we are able to designing the set of Wavelets to be orthonormal over the t-f space, with the closeness given by the ISI error metric $\mu(4)$ and the ACI error metric $\mu(5)$. ISI is the non-orthogonality error

25 between Wavelets within the same channel separated by multiples of the sampling interval 1/MT seconds where T is the sample time and M is the interval of contiguous samples. ACI is the non-orthogonality error between between Wavelets within a channel and the Wavelets in adjacent Wavelet channels at the same sample time

30 and at sample times separated by multiples of the sample interval. As observed as noise contributions within each sample in a given channel, the ISI is the noise contribution due to the other received Wavelets at the different timing offsets

22

corresponding to multiples of the sampling interval. Likewise, the ACI is the noise contribution due to the other Wavelets in adjacent Wavelet channels at the same sampling time and at multiples of the sampling interval.

5   Equations (8) step **1** ISI and ACI errors are fundamentally caused by different mechanisms and therefore have separate metrics and weights to specify their relative importance to the overall sum of the LS metrics.   ISI is a measure of the non-orthogonality between the stream of Wavelets within a channel as
10   per the construction in FIG. 4.   On the other hand, ACI is a measure of the non-orthogonality between the Wavelets within a channel and the other Wavelets in adjacent channels. This means the stopband performance metric has a significant impact on the ACI due to the sharp rolloff in frequency of the adjacent
15   channel, and the ACI metric is then a measure of the residual non-orthogonality due to the inability of the stopband rolloff in frequency from completely eliminating the ACI errors.

Equations (8) step **2** defines the weights of the LS error metrics when summed to yield the cost function J. These weights
20   are real and normalized to sum to unity. They have proven to be helpful in the Wavelet design to emphasize the relative importance of the individual error metric contributions to J.

Equations (8) step **3** defines the cost function J as the weighted sum of the LS error metrics and which is minimized with
25   respect to the DFT frequency design harmonics $\{\psi(k')\}$ to select the best LS choice for the $\{\psi(k')\}$ to design the mother Wavelet in **3** in equations (7) and the channel Wavelets by frequency translation in **5** in equations (6).

Multi-scale mother Wavelet frequency response in FIG. 5 is
30   evaluated by implementing the LS design algorithms in reference [2] that minimize the J in **3** in equations (8) to find the best set of DFT frequency design coordinates $\{\psi(k')\}$ which give the mother Wavelet **3** in equations (7). FIG. 5 plots the PSD frequency response for the multi-scale mother Wavelet and the

23

square-root (sq-rt) raised-cosine (r-c) waveforms with excess bandwidth α= 0.22, 0.40 which waveformns are extensively used for the third generation 3G CDMA communications as well as for other communications. Plotted are the measured PSD in dB **33** versus the frequency offset **34** from dc expressed in units of the symbol rate   Plotted against the normalized frequency offset are the mother PSD for the new waveform **35,** the sq-rt r-c with α=0.22 **36,** the sq-rt r-c with α=0.40 **37,** passband template for the dc filter and the stopband template for the contiguous filter, and the Nyquist rate equal to the multi-resolution complex Wavelet rate = 0.5 in units of the symbol rate.   It is believed that the multi-resolution complex Wavelets can be designed as a filter with better performance parameters than possible with any other known algorithm.

OWDMA encoding for the transmitter is defined in equations (9). Step **1** lists parameters and definitions and step **2** defines the transmitted OWDMA encoded baseband signal z(i) for contiguous data blocks and where the symbol offsets Δ account for symbol overlaps over the symbol q data block interval within each channel.

OWDMA encoding for transmitter   **(9)**

1 Parameters and definitions

   h(i) = roofing filter impulse response in time
       for h(f) in **15** in FIG.3

   ψ(i) = ψ(i|p=0,q=0,k=0) mother Wavelet in **3**
       in equations (7)
      = baseband or dc k=0 Wavelet at p=0,q=0

   N = number of OWDMA filters over the 1/T
       frequency band

   1/T = digital sample rate for OWDMA
      ≥ complex Nyquist rate for roofing filter h(f)

   NT = OWDMA Wavelet spacing

   1/NT = OWDMA Wavelet output rate

$$= \text{OWDMA Wavelet channel separation}$$

NBT $= $ channels used for data and pilot

where B is the frequency band in FIG. 3

$N(1-BT) = $ guard band channels for rolloff

of the $h(f)$

$d(k,q) = $ data modulation for user k for data block q

$= $ encoded amplitude $A(k|q)$ and phase $\varphi(k|q)$

$x(k|q) = $ transmitted symbol encoded with $d(k)$

$= A(k|q)\ \exp(j\varphi(k|q)\ )$

Assume the $h(f)$ is flat over the passband for

both Tx and Rx and can be neglected

2 Transmitted OWDMA encoded baseband signal $z(i)$

Time index field referenced to $q=0$

$i\ =\ 0,\ +/-1,\ +/-2,\ .\ .\ .$

$= $ digital sampling time index

$i_0 = $ index over a $\psi(i)$ spacing interval

$= 0,1,2,.\ .\ .\ .\ .,N-1$

$\Delta\ =$ index over the $\psi(i)$ range in units

of the $\psi(i)$ spacing interval N

$= (L/2-1),\ldots,-1,0,+1,\ldots,+(L/2-1)$

Complex baseband signal

$z(i_0|q) = $ complex baseband signal over i_0

for data block q

$= \text{FWT}[\ x(k|q+\Delta)\ ]$

$= N^{-1}\ \Sigma_\Delta\ \Sigma_k\ x(k|q+\Delta)\ \psi(i|q+\Delta,k)$

$= N^{-1}\ \Sigma_\Delta\ \Sigma_k\ x(k|q+\Delta)\ \psi(i_0+\Delta N)\ E^*(k,i_0)$

$z(i)\qquad = \Sigma_q\ z(i_0|q)$

where FWT is the fast multi-resolution complex

Wavelet transform

3 **FWT algorithm for OWDMA encoding in the transmitter**

3.a) **FWT pre-calculation FFT^{-1}**

$\lambda(i_0,q+\Delta)\ =\ N^{-1}\ \Sigma_k\ x(k|q+\Delta)\ E^*(k,i_0)$

$= \text{FFT}^{-1}[\ N^{-1}\ \Sigma_k\ x(k|q+\Delta)\ E^*(k,i_0)\ ]$

3.b) FWT post-sum

$$z(i_0|q) = \Sigma_\Delta \, \psi(i_0+\Delta N) \, \lambda(i_0|q+\Delta)$$

4 Computational complexity of fast algorithm

Real multiply rate R_M

$$R_M T = 2 \, \log_2(N) + 2 \, L$$

Real add rate R_a

$$R_A T = 3 \, \log_2(N) + 2 \, L$$

Step **3** is the new fast FWT algorithm in this invention disclosure for the transmitted OWDMA which consists of the pre-calculation FFT^{-1} in sub-step **3.a** followed by a post-sum in sub-step **3.b**.

Step **4** evaluates the real multiply complexity metric $R_M T$ and real add computational complexity metrics $R_A T$ in terms of multiplies/adds per digital sample for the fast algorithm in step **3**. The first term in these metrics is the complexity of the FFT^{-1} for a base 2 and the second term is the complexity of extending the multi-resolution complex Wavelet waveform over L of the symbol intervals.

OWDMA decoding for the receiver is defined in equations (10). Step **1** refers to **1,2** in equations (9) for the parameters and definitions and defines the OWDMA filtering Wavelet. Step **2** demonstrates Wavelet orthogonality. Estimates of the transmitted symbols in step **3** are equal to the FWT^{-1} of the received baseband signal.

OWDMA decoding for receiver (10)

1 Parameters and definitions are defined in **1,2** in

equations (9) together with

OWDMA filtering wavelet from **5** in equations (6)

$$\psi^*(i|q,k) = \psi^*(i|p=0,q,k)$$

$$= \psi(i-qN)E(k,i_0)$$

Assume the h(f) is flat over the passband for

26

both Tx and Rx and can be neglected

2 Multi-resolution complex Wavelet orthogonality from **4** in
equations (6)

    k,k' orthogonality

5
$$\Sigma_i \, \psi(i \,|\, q,k) \; \psi^*(i \,|\, q,k')$$

$$= \Sigma_i \, \psi^2(i-qN) \, E^*(k,i) \, E(k',i)$$

$$= \Sigma_{i0} \, \Sigma_\Delta \, [\Sigma_{\Delta q} \, \psi^2(i_0+\Delta)N)] \; E^*(k,i_0) \, E(k',i_0)$$

$$\cong \Sigma_{i0} \, [\; 1 \;] E^*(k,i_0) \; E(k',i_0)$$

$$= N \, \delta(k-k')$$

10
    using the completeness property of the
multi-resolution complex Wavelet from reference [2]

$$[\Sigma_\Delta \, \psi^2(i_0 + \Delta)N)] \cong 1 \text{ for all } i_0$$

    q,k and q',k' orthogonality proven in reference
[2] and restated in **4** in equations (6)

15
3 OWDMA decoding derives estimates $\hat{x}(k|q)$ of $x(k|q)$ for
data block q from the receiver estimates $\hat{z}(i)$ of $z(i)$

$$\hat{x}(k|q) \;=\; FWT^{-1}[\; \hat{z}(i) \;]$$

$$= \Sigma_i \, \hat{z}(i) \, \psi^*(i|q,k)$$

4 FWT algorithm for OWDMA decoding in receiver

20
    4.a) FWT pre-sum

$$\lambda(i_0|q) \;=\; \Sigma_\Delta \, \hat{z}(i_0|q+\Delta) \, \psi(i_0+\Delta N)$$

$$= \Sigma_\Delta \, \hat{z}(i_0+\Delta N|q) \, \psi(i_0+\Delta N)$$

    4.b) FWT pre-sum FFT

$$\hat{x}(k|q) = \Sigma_{i0} \, \lambda(i_0|q) \, E(k,i_0)$$

25
5 Computational complexity of fast algorithm

    Real multiply rate R_M

$$R_M T = 2 \, \log_2(N) + 2 \, L$$

    Real add rate R_a

$$R_A T = 3 \, \log_2(N) + 2 \, L$$

30

Step **4** is the new fast algorithm for the received OWDMA
which partitions the baseband symbol detection $\hat{x}(k|q)$ in step **3**

into a pre-sum calculation sub-step **4.a** of $\lambda(i_0|q)$ followed by a sub-step **4.b** FFT of this pre-sum.

Step **5** evaluates the real multiply complexity metric R_MT and real add computational complexity metrics R_AT in terms of multiplies/adds per digital sample for the fast algorithm in step **3**. The first term in these metrics is the complexity of the FFT^{-1} for a base 2 and the second term is the complexity of extending the multi-resolution complex Wavelet waveform over L of the symbol intervals.

MS-CDMA parameters and codes are defined in equations (11). Step **1** defines the scenario parameters. Step **2** partitions the user index u field into the sub-fields u_0, u_1 of size N_0, N_1 for scales 0,1 respectively and which are the indices over the users within each channel and the indices over the channels within the MS-CDMA group and which uniquely represent u as $u = u_0 + u_1 N_1$.

Step **3** partitions the code chip index n field into the sub-fields n_0, n_1 of size N_0, N_1 for scales 0,1 respectively and which are the indices over the chips within each channel and the indices over the channels of the MS-CDMA group and which uniquely represent n as $n = n_0 + n_1 N_1$.

Step **4** defines the $N_c \times N_c$ MS-CDMA code matrix C whose elements are $C(u,n)$ where $u+1$ is the row index and $n+1$ is the column index and where the $+1$ has been added to correspond to the row and column numbering starting with $+1$. MS-CDMA code vector

MS-CDMA parameters and codes (11)

1 Scenario parameters

M   = number of communications channels
        of band B

N_0 = number of CDMA chips per channel

N_1 = number of channels in MS-CDMA group

N_c = number of chips in MS-CDMA group = $N_0 N_1$

$1/T_0$ = MS-CDMA chip/symbol rate

        = $1/NT$ for OFDMA,OWDMA   in FIG. 1,2

28

```
x(u,q) = User u in group q
       = x(k|q)    when $N_0$=1, u=k
       = x(k)      when $N_0$=1, u=k, q=0
```

2   User index u for a MS-CDMA group

```
u   = Index of CDMA users
    = 0,1,…, ($N_c$-1)
    = ($u_0$,$u_1$)    field representation of u
    = $u_0$ + $u_1 N_0$    for fields $u_0$, $u_1$
```

where the index fields are

```
$u_0$   = index of users in a channel in
          the MS-CDMA group
      = 0,1,…, ($N_0$-1)
$u_1$   = index of channels in the MS-CDMA group
      = 0,1,…,$N_1$-1
```

3   Code chip index n for a MS-CDMA group

```
n   = Index of CDMA code chips
    = 0,1,…, ($N_c$-1)
    = ($n_0$,$n_1$)    field representation of n
    = $n_0$ + $n_1 N_0$ for fields $n_0$, $n_1$
```

where the index fields are

```
$n_0$   = index of code chips within a channel
          in the MS-CDMA group
      = 0,1,…, ($N_0$ -1)
$n_1$   = index of channels in the MS-CDMA group
      = 0,1,…, ( $N_1$-1)
```

4   MS-CDMA code matrix C for a MS-CDMA group

```
C    = $N_c$ x $N_c$ MS-CDMA code matrix
     = [C(u,n)]    matrix of elements {C(u,n)}
     = [c(u)]    matrix of 1x $N_c$ code vectors
C(u) = MS-CDMA code vector u which is row u+1 in
       C counting rows,columns starting with 1
     = [C(u,0), C(u,1),  . . . ,C(u, $N_c$-1)]
```

5   Kronecker product example for C for a MS-CDMA group

```
C    = $C_1 \otimes C_0$  Kronecker product of $C_1$ and $C_0$
```

29

$$= [\ C(u,n) = C_1(u_1,n_1)\,C_0(u_0,n_0)\ ]$$

where

$\otimes$ $\quad$ = Kronecker product of C_1 and C_0

C_1 $\quad$ = N_1 x N_1 MS-CDMA scale 1 code matrix

$\quad$ = $[C_1(u_1,n_1)]$ $\quad$ matrix of elements $\{C_1(u_1,n_1)\}$

$\quad\quad$ over the user channels within the group

C_0 $\quad$ = N_0 x N_0 MS-CDMA scale 0 code matrix

$\quad$ = $[C_0(u_0,n_0)]$ matrix of elements $\{C_1(u_1,n_1)\}$

$\quad\quad$ over the user chips within each channel

$\quad\quad$ in the group

c(u) for user u is the row u+1 of C. The C is a complex orthogonal code matrix.

Step **5** is an example of a MS-CDMA code matrix C which is factorable into a Kronecker product $C=C_1\otimes C_0$ of C_1 and C_0 where "$\otimes$" is the Kronecker product and the matrix C_1 is the N_1 x N_1 MS-CDMA scale 1 code matrix over the user channels within the MS-CDMA group and the matrix C_0 is the N_0 x N_0 MS-CDMA scale 0 code matrix for the user chips within each channel in the MS-CDMA group.

A general definition for MS-CDMA code matrix C which includes the definitions in references [3],[4] is allowed by this invention disclosure. The example Kronecker product construction of C is important because it is a property possessed by the real Walsh or Hadamard orthogonal matrices as well as the majority of orthogonal matrices used or proposed for CDMA and because of the relative ease in finding a fast algorithm for the transmitter and receiver coding and decoding and because of the ease in constructing multiple scales for MS-CDMA as demonstrated in **5** in equations (11).

MS-CDMA representative application to OFDMA in FIG. 1 uses the candidate architecture which spreads the CDMA over the M contiguous 48 data channels or 52 contiguous data plus pilot channels and the representative application to OWDMA in FIG. 3

30

uses the candidate architecture which spreads the CDMA over the M contiguous OFDMA communications channels across B.

MS-CDMA partitions the M channels into channel groups of size N_1 and provides a scale over the chips within the channels and another scale over the channels within this group. Code chip length N_c for each user in a channel group is equal to $N_c = N_0 N_1$ where N_0 is the number of chips in each channel assigned to scale "0" and N_1 is the number of channels assigned to scale "1" within the group. Each user has a chip scale "0" and a channel scale "1" . Chip scale "0" spreads the data over the chips within each channel and channel scale "1" then spreads the channel chips uniformly over the N_1 channels with the result that each user occupies each of the channels within the N_1 channel group.

There could be from 1 to M/N_1 channel groups depending on the architecture and applications. The use of multiples groups $M/N_1 > 1$ tends to be desirable since the storage requirements and computational complexity are reduced as the number of groups are increased and the spreading advantages within each group tend to saturate as the number $N_1 > 16$ when the channels within each goup are spread across the fullband M channels.

For $N_0 = 1$ there is no CDMA within each channel and the MS-CDMA then spreads the signals over each channel within a group for both OFDMA and OWDMA to function as a means to spread each channel over the fullband M channels and which may be a desirable architecture when the channels are sufficiently narrow to produce a sufficiently long pulse to counter multipath.

MS-CDMA OFDMA transmitter equations are defined in equations (12) for MS-CDMA. Step **1** gives the parameters and definitions. Step **2** defines the encoding equations for chip n_0 for data block q. Sub-step **2.a** uses the fast code transform FCT developed in references [3],[4] to generate the encoded vector. Sub-step **2.b** uses the inverse FFT^{-1} to construct the transmitter complex baseband signal $z(i_0|n_0+qN_0)$ for chip n_0 for data block q and these signals are combined in sub-step **2.c** to generate the transmitter signal $z(i)$ for all n_0, q.

31

Step **3** evaluates the real multiply complexity metric R_MT and real add computational complexity metrics R_AT in terms of multiplies/adds per digital sample for the fast algorithm in step **3**. The first term in these metrics is the complexity of the FFT^{-1}

5

MS-CDMA OFDMA transmitter equations (12)

1 Parameters and definitions are defined in **1** in
equations (2),(9),(11) together with
MS-CDMA group index field {g}

10      $g = 0,1,. . . ,(M/N_1-1)$ where M/N_1 = number
         of MS-CDMA groups over the M data channels
Frequency harmonic k
    $k = k(n_1|g,q)$
MS-CDMA chip index fields

15     $n = n_0 + n_1N_0$
     $= 0,1,2,. . ,N_c-1$
    $n_0 = 0,1,2,. . ,N_0-1$ scale 0 chips in channel
    $n_1 = 0,1,2,. . ,N_1-1$ scale 1 chips over channels
    $N_c = N_0N_1$ number of chips in a MS-CDMA group

20 MS-CDMA channel code index n_1
    $n_1 = n_1(k|g,q)$ function of k for a given g,q
User symbol x
    $x = x(u|g,q)$
     $= A(u|g,q) \exp j\varphi(u|g,q)$

25 MS-CDMS code orthogonality
    $CC^* = N_c I$
PN spreading code P(n) for chip n in group g
    $P(n|g,q) = \exp(j\varphi(n|g,q)$
Assume the band and pulse filtering can be

30   neglected on both Tx and Rx which is
     equivalent to the assumption $\underline{p}(i) \cong 1$ for all i

2 MS-CDMA OFDMA encoding for complex baseband signal z(i)

2.a) FCT MS-CDMA encoding for data block q
    $Z(n|g,q) = FCT[x(u|g,q)]$

32

$$= N_c^{-1} \Sigma_u x(u|g,q) C(u,n) P(n|g,q)$$

where FCT is the fast code transform

2.b) FFT^{-1} OFDMA encoding for chip n_0 of data block q

$$z(i_0|n_0+qN_0) = FFT^{-1} [Z(n|g,q)]$$

$$= N^{-1} \Sigma_k Z(n|g,q) E^*(k,i_0)$$

where $n = n_0 + n_1N_0$

$$n_1 = n_1(k|g,q)$$

$$Z(n|g,q) = Z(n_0+n_1(k|g,q)N_0)$$

2.c) Complex baseband transmitter signal z(i)

$$z(i) = \Sigma_{(o)} z(i_0|n_0+qN_0) \quad \text{for } (o)=(n_0+qN_0)N$$

3 Computational complexity

Real multiply rate R_M

$$R_MT = 2 \log_2(N)$$

Real add rate R_a

$$R_AT = 3 \log_2(N) + 2 \log_2(N_c) + 2$$

for a base 2 and the second term is the complexity of the FCT assuming the FCT does not require any multiplies.

MS-CDMA OWDMA transmitter equations are defined in equations (13) for MS-CDMA. Step **1** lists the parameters and definitions. Step **2** defines the encoding equations for chip n_0 for data block q. The FCT on the symbols in sub-step **2.a** yields the encoded data block $Z(n|g,q)$ and the FWT on this output in sub-step **2.b** yields the transmitter complex baseband signal $z(i_0|n_0+qN_0)$ for chip n_0 for data block q and these signals are combined in sub-step **2.c** to generate the transmitter signal z(i) for all n_0,q.

MS-CDMA OWDMA transmitter equations (13)

1 Parameters and definitions are defined in **1** in
equations (9),(12) together with the range of q

q = 0 for the data block being addressed

= +/-1 contiguous data blocks

Assume the h(f) is flat over the passband for

both Tx and Rx and can be neglected

2 MS-CDMA OWDMA encoding for chip n_0 for data block q

2.a) FCT MS-CDMA encoding for data block q

$$Z(n|g,q) = FCT[x(u|g,q)]$$

$$= N_c^{-1} \Sigma_u x(u|g,q) C(u,n) P(n|g)$$

2.b) FWT OWDMA encoding for chip n_0 of data block q

$$z(i_0|n_0+qN_0) = \Sigma_{\delta q} \Sigma_\Delta FWT[Z(n+\Delta|g,q+\delta q)]$$

$$= N^{-1} \Sigma_k \Sigma_{\delta q} \Sigma_\Delta Z(n+\Delta|g,q+\delta q) \psi(i|n_0+\Delta,k)$$

$$= N^{-1} \Sigma_k \Sigma_{\delta q} \Sigma_\Delta Z(n+\Delta|g,q+\delta q) \psi(i_0+\Delta N) E^*(k,i_0)$$

where the overlap conditions on δq are

$$\delta q = \Delta \quad \text{for } N_0=1$$

$$= sign(\Delta+n_0)\lfloor |\Delta+n_0|/N_0 \rfloor \quad \text{otherwise}$$

$$sign(o) = \text{numerical sign of (o)}$$

$$\lfloor (o) \rfloor = \text{rounded down integer value of (o)}$$

where the overlap index $\Delta = 0, +/-1,$.

$$. . ., +/-(L/2-1)$$

2.c) Complex baseband transmitter signal z(i)

$$z(i) = \Sigma_{(o)} z(i_0|n_0+qN_0) \quad \text{for } (o)=(n_0+qN_0) N$$

3 FWT algorithm for OWDMA encoding in the transmitter

3.a) FWT pre-calculation FFT^{-1}

$$\lambda(i_0|n_0+\Delta,q)$$

$$= N^{-1} \Sigma_k Z(n+\Delta|g,q) E^*(k,i_0)]$$

$$= FFT^{-1}[N^{-1} \Sigma_k Z(n+\Delta|g,q) E^*(k,i_0)]]$$

3.b) FWT post-sum

$$z(i_0|n_0) = \Sigma_q \Sigma_\Delta \psi(i-(n_0+\Delta) N) \lambda(i_0|n_0+\Delta,q)$$

4 Computational complexity for fast algorithms in 2.a,3

Real multiply rate R_M

$$R_M T = 2 \log_2(N) + 2 L$$

Real add rate R_a

$$R_A T = 3 \log_2(N) + 2 L + 2 \log_2(N_c) + 2$$

Step **3** is the new fast FWT algorithm in this invention disclosure for the transmitted OWDMA which consists of the pre-calculation FFT^{-1} in sub-step **3.a** followed a post-sum in sub-step **3.b** of the product from sub-step 3.a with the corresponding Wavelet overlaps over the q data block interval.

Step **4** evaluates the real multiply complexity metric R_MT and real add computational complexity metrics R_AT in terms of multiplies/adds per digital sample for the fast algorithms FCT and FWT in steps **2,3**. The first term in these metrics is the complexity of the FFT^{-1} for a base 2, the second term 2L is the complexity of extending the multi-resolution complex Wavelet waveform over L of the MT symbol intervals, and the remaining terms are the complexity of the FCT assuming the FCT does not require any multiplies.

MS-CDMA OFDMA/OWDMA encoding for the transmitter in FIG. 6 is a representative implementation of the MS-CDMA OFDMA encoding algorithms in equations (12) and the MS-CDMA OWDMA encoding algorithms in equations (13). Signal processing starts with the input stream of data encoded symbols x(u|g,q) **40** from the transmitter symbol encoder **52** in FIG. 7 and defined in **1** in equations (12) for both OFDMA and OWDMA.

FIG. 6 MS-CDMA encoding **41** implements the fast cpde tramsform FCT encoding defined in sub-step **2.a** in equations (12),(13) for the MS-CDMA encoding and PN cover or spreading encoding to generate the N_c outputs x(u|g,q)C(u,n)P(n|g) for each MS-CDMA group g and data block q. For each group these outputs are summed **42** over u to generate the encoded vector Z(n|g,q) in **43**.

OFDMA processing **44** performs an FFT^{-1} on the received set of vectors Z(n|g,q) and a summation to implement sub-steps **2.b,2.c** in equations (12) and the output is band filtered **46** to generate the MS-CDMA OWDMA encoded complex baseband signal z(i) in **47**.

OWDMA processing **45** performs an FWT on the received set of vectors Z(n|g,q) and a summation to implement sub-steps **2.b,2.c**

in equations (13) and the output is band filtered **46** to generate the MS-CDMA OWDMA encoded complex baseband signal z(i) in **47**.

Outputs $z(i_0|n_0)$ **47** from the MS-CDMA OFDMA and MS-CDMA OWDMA are digital-to-analog DAC converted **48** and handed off to the analog front end **49** as the complex baseband analog signal z(t) in **49**.

MS-CDMA OFDMA/OWDMA transmitter block diagram in FIG. 7 is a representative transmitter implementation of the MS-CDMA OFDMA and MS-CDMA OWDMA encoding in the shaded box in FIG. 6. The transmitter block diagram in FIG. 7 includes the FIG. 6 MS-CDMA OFDMA/OWDMA encoding in an abbreviated format in the shaded box **54** in FIG. 7. FIG. 7 signal processing starts with the stream of user input data words. Frame processor **51** accepts these data words and performs the encoding and frame formatting, and passes the outputs to the symbol encoder **52** which encodes the frame symbols into amplitude and phase coded symbols $x(u|g,q)$ **53** which are the input to the MS-CDMA encoding **55** and which is **41,42** in FIG. 6.

MS-CDMA FCT encoding outputs $Z(n|g,q)$ **56** are handed over to the OFDMA and OWDMA processing **57** which performs an inverse FFT^{-1} followed by a band filtering for OFDMA which is **44,46** in FIG. 4 and performs an inverse FWT^{-1} followed by a band filtering which is **45,46** in FIG.6. This complex baseband signal z(i) in **47** in FIG.6 is digital-to-analog DAC converted **59** and the the output complex baseband analog signal z(t) **60** is handed off to the analog front end **61**.

The z(t) is single sideband upconverted, amplified, and transmitted (Tx) by the analog front end **61** as the real waveform v(t) **62** at the carrier frequency f_0 whose amplitude is the real part of the complex envelope of the baseband waveform z(t) and the phase angle ϕ accounts for the phase change from the baseband signal to the transmitted signal. Output waveform **62** from the analog front end is the Tx waveform from the Tx antenna.

36

It should be obvious to anyone skilled in the communications art that this example implementation in FIG. 6,7 clearly defines the fundamental MS-CDMA OFDMA and MS-CDMA OWDMA signal processing relevant to this invention disclosure
5 and it is obvious that this example is representative of the other possible signal processing approaches.

MS-CDMA OFDMA receiver equations are defined in equations (14). Step **1** lists the parameters and definitions and the assumption that the band and pulse filtering can be
10 neglected. Step **2** defines decoding of the received chip signal to derive the estimate $\hat{x}(u|g,q)$ of the transmitted symbol $x(u|g,q)$. Sub-step **2.a** derives the estimate for the encoded symbols using the FFT and sub-step **2.b** uses the FCT^{-1} on this estimate to derive the transmitted symbol estimate.

15

MS-CDMA OFDMA receiver equations (14)

1 Parameters and definitions are defined in **1** in
equations (2),(9),(11) together with

$\hat{z}(i)$ = receiver band filter estimate of
20 the transmitted complex baseband signal $z(i)$

Assume the band and pulse filtering can be

neglected on both Tx and Rx which is

equivalent to the assumption $\underline{p}(i) \cong 1$ for all i

2 MS-CDMA OFDMA decoding to derive data symbol $\hat{x}(u|g,q)$

25 **2.a) FFT of each received chip vector** $\hat{z}(i_0|n_0+qN_0)$

$\hat{Z}(n|g,q)$ = estimate of transmitted $Z(n|g.q)$

$= FFT[\ \hat{z}(i_0|n_0+qN_0)\ ]$

$= \Sigma_{i0}\ \hat{z}(i_0|n_0+qN_0)\ E(k,i_0)$

where $\hat{z}(i_0|n_0+qN_0) = \hat{z}(i=i_0+(n_0+qN_0)N\ )$

30 **2.b) FCT^{-1} of each group g encoded vector** $Z'(n|g,q)$

$\hat{x}(u|g,q) = FCT^{-1}[\ \hat{Z}(n|g,q=0)\ ]$

$= \Sigma_n\ \hat{Z}(n|g,q)P^*(n|g)C^*(u,n)$

3 Computational complexity is the same as calculated
in 3 in equations (12) for the transmitter

MS-CDMA OWDMA receiver equations are defined in equations (15). Step **1** lists the parameters and definitions and the assumption that the band and pulse filtering can be neglected.

5

MS-CDMA OWDMA receiver equations (15)

1 Parameters and definitions are defined in **1** in

equations (2),(9),(11),(14) together with

10   $\hat{z}(i)$ = receiver band filter estimate of

   the transmitted complex baseband signal $z(i)$

Assume the $h(f)$ is flat over the passband for

  both Tx and Rx and can be neglected

2 MS-CDMA OWDMA decoding to derive data symbol $\hat{x}(u|g,q)$

15   **2.a) FWT^{-1} of each received signal** $\hat{z}(i)$

   $\hat{Z}(n|g,q)$ = estimate of transmitted $Z(n|g.q)$

    = FWT^{-1}[$\hat{z}(i)$]

    = $\Sigma_i \, \hat{z}(i)\psi^*(i|q,k)$

    = $\Sigma_{i0} \, \Sigma_\Delta \, \hat{z}(i_0|n_0+(q+\Delta)N)\psi(i_0+\Delta N)E(k,i_0)$

20   where $\hat{z}(i_0|n_0+qN_0)$ = $\hat{z}(i=i_0+(n_0+qN_0)N)$

    $k \rightarrow g$ which means k specifies g

    $n_0, k \rightarrow n=n_0+n_1(k|g,q)$

  2.b) FCT^{-1} of each group g encoded vector $Z(n|g,q)$

   $\hat{x}(u|g,q)$ = FCT^{-1}[$\hat{Z}(n|g,q)$]

25   = $\Sigma_n \, \hat{Z}(n|g,q)P^*(n|g)C^*(u,n)$

3 FWT^{-1} algorithm

  2.a) FWT^{-1} pre-sum

   $\lambda(i_0|g,q)$ = $\Sigma_\Delta \, \hat{z}(i_0|n_0+(q+\Delta)N)\psi(i-(n_0+\Delta)N)$

   where $n_0+\Delta \rightarrow g$ using the boundary conditions

30   in 2.b in equations (13)

  2.b) FWT^{-1} pre-sum FFT

   $\hat{Z}(n|g,q)$ = Σ_{i0} FFT[$\lambda(i_0|g,q)$]

    = $\Sigma_{i0} \, \lambda(i_0|g,q)E(k,i_0)$

3 Computational complexity is the same as calculated in 3 in equations (13) for the transmitter

Step **2** defines decoding of the received chip signal to derive the estimate $\hat{x}(u|g,q)$ of the transmitted symbol $x(u|g,q)$. Sub-step **2.a** derives the estimate for the encoded symbols using the FWT^{-1} and sub-step **2.b** uses the FCT^{-1} on this estimate to derive the transmitted symbol estimate. Step **3** is the new fast FWT algorithm in this invention disclosure for the received MS-CDMA OWDMA which consists of the pre-sum in sub-step **3.a** followed an FFT on this pre-sum.

MS-CDMA OFDMA/OWDMA decoding for the receiver in FIG. 8 is a representative implementation of the MS-CDMA OFDMA decoding algorithms in equations (14) and the MS-CDMA OWDMA decoding algorithms in equations (15). Signal processing starts with the input intermediate frequency IF signal after being single sideband downconverted and synchronized in frequency **63** from the receiver front end **72** in FIG. 9. This input signal is band filtered **64** and handed off to the analog-to-digital converter ADC or A/D **65** whose digital output is the received estimate $\hat{z}(i)$ **66** of the transmitted complex baseband signal $z(i)$ **60** in FIG. 7. For OFDMA **67** this received signal is processed by an FFT to derive estimates $\hat{Z}(n|g,q)$ **68** of the MS-CDMA encoded signal $Z(n|g,q)$ **56** in FIG. 7. For OWDMA **67** this received signal is processed by an inverse multi-resolution complex Wavelet transform FWT^{-1} to derive estimates $\hat{Z}(n|g,q)$ **68** of the MS-CDMA encoded signal $Z(n|g,q)$ **56** in FIG. 7 implementing the fast algorithm defined in **2** in equations (15). Recovered estimates $\hat{Z}(n|g,q)$ **68** are processed by the inverse fast code transform FCT^{-1} **69** to derive estimates $\hat{x}(u|g,q)$ **70** of the transmitted data symbols $x(u|g,q)$ **53** in FIG. 7 for hand over to the symbol decoder.

MS-CDMA OFDMA/OWDMA receiver block diagram in FIG. 9 is a representative receiver implementation of the MS-CDMA OFDMA and

MS-CDMA OWDMA decoding in the shaded box in FIG. 8. The receiver block diagram in FIG. 9 includes the FIG. 8 MS-CDMA OFDMA/OWDMA decoding in an abbreviated format in the shaded box **74** in FIG. 9. FIG. 9 signal processing starts with the received Rx waveform

5   **71** from the transmitter **62** in FIG. 7. Received signal $\hat{v}(t)$ **71** is an estimate of the transmitted signal $v(t)$ **62** in FIG. 7 received with errors in time Δt, frequency Δf, phase $\Delta\theta$, and with an estimate $\hat{z}(i)$ of the transmitted complex baseband signal $z(t)$ **60** in FIG. 7. This received signal $\hat{v}(t)$ is amplified and

10 downconverted by the analog front end **72** and single side band SSB downconverted and synchronized **73** and handed over to the digital-to-analog conversion DAC processing **75** for band filtering by $h(f)$ and digitization to generate the baseband signal $\hat{z}(i)$ **76** which is the received estimate of the transmitted signal $z(i)$ 60

15 in FIG. 7. Timing synchronization could be implemented in the DAC.

Outputs $\hat{z}(i)$ are processed by the MS-CDMA OFDMA/OWDMA decoding to derive estimates $\hat{x}(u|g,q)$ **79** of the transmitted symbols $x(u\}g,q)$ **53** in FIG. 7 and part of the information is

20 handed off to the synchronization (sync) processor. For the inverse MS-CDMA^{-1} OFDMA^{-1} the processing **79** consists of the FFT to recover estimates $\hat{Z}(n|g,q)$ of $Z(n|g,q)$ followed by an inverse FCT^{-1} to recover $\hat{x}(u|g,q)$. For the inverse MS-CDMA^{-1} OWDMA^{-1} the processing **79** consists of the inverse FWT^{-1} to recover estimates

25 $\hat{Z}(n|g,q)$ of $Z(n|g,q)$ followed by an inverse FCT^{-1} to recover $\hat{x}(u|g,q)$ and the FWT^{-1} implementes the fast transform in **2** in equations (15). Outputs $\hat{x}(u|g,q)$ are processed by the symbol decoder **80** and the frame processor **81** for handoff as the received Rx data **82**.

30 It should be obvious to anyone skilled in the communications art that this example implementation in FIG. 8,9 clearly defines the fundamental MS-CDMA OFDMA and MS-CDMA OWDMA signal processing relevant to this invention disclosure

and it is obvious that this example is representative of the other possible signal processing approaches.

Variable power control across the frequency band can be implemented by assigning each group g of transmit Tx signals their own power level P(g). Each MS-CDMA group g occupies a subset of the channels over the frequency band B consisting of N_1 channels which means that the users within group g are transmitted with the same Tx power. On receive each group g of channels is processed separately so there is no cross-talk between the users in the different groups. The OWDMA was designed to support large dynamic range imbalances between channels which could be present with power level control. MS-CDMA OFDMA/OWDMA variable power control over the frequency subbands corresponding to the MS-CDMA groups supports the potential for diversity improvements by allocation of the available power to emphasize the 'best' set of available subbands, which subbands are not required to be contiguous as well as supporting the simultaneous support of multiple users with differing power requirements due to range, multi-path, and path attenuation effects.

A second configuration for variable power control is described in reference [2] and increases the flexibility of power control to all of the individual channels.

Preferred embodiments in the previous description is provided to enable any person skilled in the art to make or use the present invention. The various modifications to these embodiments will be readily apparent to those skilled in the art, and the generic principles defined herein may be applied to other embodiments without the use of the inventive faculty. Thus, the present invention is not intended to be limited to the embodiments shown herein but is not to be accorded the wider scope consistent with the principles and novel features disclosed herein.

REFERENCES

[1] IEEE 802.11g standard

[21 Patent filed 09/826,118 01/09/2001 New multi-resolution waveforms, U.A. von der Embse

[3] Patent filed 29/143,845 01/09/2001 Multi-scale CDMA, U.A. von der Embse

[4] Patent filed 09/826,117 01/09/2001 Hybrid-Walsh codes for CDMA, U.A. von der Embse

[5] "Multirate Digital Signal Processing", R.E. Crochiere, L.R. Rabiner, 1983, Prentice-Hall

[6] "Multirate Systems and Filter Banks", R.P. Vaidyanathan, 1993, Prentice-Hall

[7] "Wavelets and Filter Banks", Gilbert Strang, Truong Nguyen, 1996, Wellesley-Cambridge Press

[8] Ronald R. Coifman, Yves Meyer, Victor Wickerhauser, "Wavelet analysis and signal processing", in "Wavelets and Their Applications', Jones & Bartlett Publishers, 1992

[9] T. Blu, "A new design algorithm for two-band orthonormal rational filter banks and orthonormal rational Wavelets", IEEE Signal Processing, June 1998, pp. 1494-1504

[10] M. Unser, P. Thevenaz, and A. Aldroubi, "Shift-orthogonal Wavelet bases", IEEE Signal Processing, July 1998, pp. 1827-1836

[11] K.C. Ho and Y. T. Chan, "Optimum discrete Wavelet scaling and its application to delay and Doppler estimation", IEEE Signal Processing, Sept. 1998, pp. 2285-2290

[12] I. Daubechies, "Ten Lectures on Wavelets", Philadelphia: SIAM, 1992

[13] P.P. Vaidyanathan and T.Q. Nguyen, "Eigenvalues: A New Approach to Least-Squares FIR Filter Design and Applications Including Nyquist Filters", IEEE Trans. on Circuits and Systems, Vo. CAS-34, No. 1, Jan. 1987, pp 11-23

[14] J.H. Mc.Clellan, T.W. Parks and L.R. Rabiner, "A Computer Program for Designing Optimum FIR Linear Phase Filters', IEEE Trans Audio Electroacoust. Vol. AU-21, Dec. 1973, pp. 506-526